GaAsSb/ InAlAs PA DHBTs Grown by Production MBE

Zhu H J†, Kuo J M, Pinsukanjana P, Vargason K, Herrera M, Ontiveros D, Boehme C, and Kao Y C

(Intelligent Epitaxy Technology, Inc., Richardson, TX 75081, USA)

Abstract: The epi material growth of GaAsSb based DHBTs with InAlAs emitters are investigated using a 4 × 100mm multi-wafer production Riber 49 MBE reactor fully equipped with real-time in-situ sensors including an absorption band edge spectroscope and an optical-based flux monitor. The state-of-the-art hole mobilities are obtained from 100nm thick carbon-doped GaAsSb. A Sb composition variation of less than ±0.1 atomic percent across a 4 ×100mm platen configuration has been achieved. The large area InAlAs/ GaAsSb/ InP DHBT device demonstrates excellent DC characteristics, such as $BV_{CEO} > 6V$ and a DC current gain of 45 at $1kA/cm^2$ for an emitter size of 50μm ×50μm. The devices have a 40nm thick GaAsSb base with p-doping of $4.5 \times 10^{19} cm^{-3}$. Devices with an emitter size of 4μm ×30μm have a current gain variation less than 2% across the fully processed 100mm wafer. f_t and f_{max} are over 50GHz, with a power efficiency of 50%, which are comparable to standard power GaAs HBT results. These results demonstrate the potential application of GaAsSb/ InP DHBT for power amplifiers and the feasibility of multi-wafer MBE for mass production of GaAsSb-based HBTs.

Key words: InP; GaAsSb; DHBT; MBE; multi-wafer production; in-situ sensors
EEACC: 2520D; 2520Z
CLC number: TN325⁺.3 **Document code:** A **Article ID:** 0253-4177(2006)04-0635-06

1 Introduction

InP/ InGaAs-based DHBTs have demonstrated excellent microwave characteristics for OC-768 communication system applications. However, a complicated collector-base design is required to overcome the collector current blockage problem resulting from the type I band alignment between the InGaAs base and InP collector. When the conventional InGaAs base is replaced with GaAsSb, the type II band alignment (staggered) between InP and $GaAs_{0.51}Sb_{0.49}$ permits the use of a single InP layer as the collector without the problem of collector current blockage[1~3]. Therefore InP/ GaAsSb/ InP DHBTs simplify device design and have high breakdown voltages, low offset and knee voltages, and extremely high current driving capability. Recent MOCVD-grown DHBT results with abrupt InP/ GaAsSb/ InP heterojunctions have demonstrated f_t and f_{max} values as high as 300GHz at high current densities[4]. InP has typically been the preferred emitter material for InP/ GaAsSb DHBTs for its superior etching selectivity. However, the negative conduction band discontinuity between the InP emitter and the GaAsSb base is an inherent disadvantage of an InP/ GaAsSb emitter-base junction. In addition, it has been difficult to grow good InP on GaAsSb by MBE. Therefore, it is important to explore different emitter material design for MBE. Moreover, because GaAsSb is a mixed group V compound semiconductor, good composition uniformity has been difficult to achieve even with small single wafer MBE systems, let alone large multi-wafer system.

Multi-wafer growth of uniform GaAsSb with a proper emitter material is the key for the success of InP/ GaAsSb/ InP DHBT technology.

In this paper, we first demonstrate highly uniform GaAsSb across a 100mm wafer with state-of-the-art hole mobility using a 4 ×100mm multi-wafer MBE reactor. Then we will discuss the details of the use of various emitter materials for the growth of GaAsSb/ InP DHBTs based on band lineup considerations and growth-related issues. Finally, large and small area device characteristics from these GaAsSb/ InP power amplifier DHBTs will be presented. Various circuits will be used to

† Corresponding author. Email: zhu@intelliEPI.com
Received 4 January 2006
©2006 Chinese Institute of Electronics

compare power performance and current carrying capability. Results will be discussed in the end.

2 Experiment

The epi materials are grown using a multi-wafer Riber 49 MBE system. The reactor is equipped with Al, Ga, and In solid source effusion cells for group Ⅲ elements and As, P, and Sb valve crackers for group Ⅴ elements. Silicon is used for the n-type dopant, and a gas source CBr_4 for p-type dopant. The epi-ready InP substrate was used in this paper. The optimal growth conditions are obtained by systematically varying the substrate temperature, total group Ⅴ pressure, and As/Sb flux ratio. The wafers are heated to 520 ℃ for thermal removal of the oxidation layer before growth. The growth temperature is measured by absorption band edge spectroscopy (ABES)[5,6]. The group Ⅲ fluxes are monitored by an optical-based flux monitor (OFM)[7,8].

For GaAsSb material characterization, 100nm thick carbon-doped GaAsSb was grown on (100) semi-insulating InP : Fe substrates. Carrier concentration and mobility were measured with a Hall setup. GaAsSb material composition was characterized with double crystal X-ray diffraction in the (400) orientation.

The steps of the DHBT large area device (LAD) fabrication consist of emitter and base etching followed by Ti/Au non-alloy ohmic evaporation. The LAD measurements were taken from devices with a 50μm ×50μm emitter. The small area devices (SAD) with a size of 4μm ×30μm were fabricated by a commercial GaAs foundry. RF tests were performed on un-thinned wafers.

3 Results and discussion

3.1 Sb cracker setup and its stability

Figure 1 shows Sb flux versus valve position measured initially and repeated several times during a period of several months. As we can see, the flux profile is not as linear as for the As or P cracker cells. Even after several months, the Sb flux still falls onto the same calibration curve, indicating that the Sb flux is reproducible and controllable.

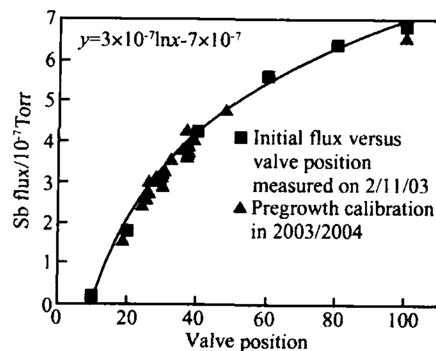

Fig. 1 Sb flux versus valve position of Sb cracker measured at different dates The fluxes measured at different times fall into one line, which means the flux is very reproducible.

3.2 Determination of growth conditions

In order to find conditions in which the Sb composition can be easily controlled, first we fix the Ga growth rate and find the lattice matching conditions at a low temperature (400 ℃) with the adjustment of As and Sb fluxes. Then we evaluate the effect of substrate growth temperature at fixed As and Sb flux rates by X-ray diffraction. The plot of Sb composition versus temperature is shown in Fig. 2. Sb composition remains almost unchanged below 460 ℃. The Sb starts to desorb at about 455 ℃, so we keep the growth temperature of the GaAsSb below 455 ℃. Figure 3 shows the PL intensity versus growth temperature. During this se-

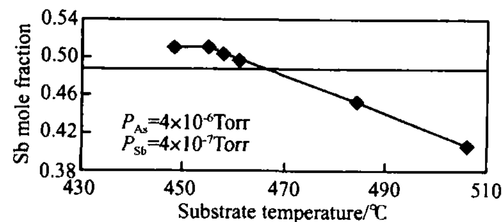

Fig. 2 Dependence of Sb composition in GaAsSb on the growth temperature Sb composition in GaAsSb is very stable until the temperature exceeds 455 ℃

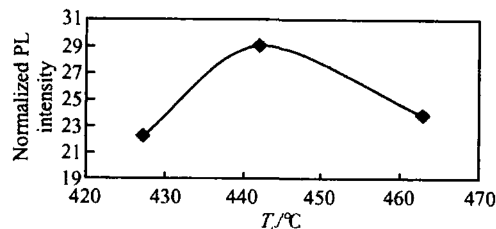

Fig. 3 PL intensity of GaAsSb doped with carbon at different substrate growth temperatures Growth temperature of 440 ℃ produces the brightest PL, which indicates the best crystal quality.

ries of tests ,the growth temperature changes while the doping level and Sb composition are controlled as closely as possible. Peak PL intensity was observed around 440 ℃, which means the highest crystal quality is achieved at that temperature. Thus ,we use 440 ℃ for the GaAsSb growth temperature. Then the Hall mobility is measured at different carbon doping concentrations while maintaining lattice matching conditions. The X-ray diffraction peak position for the $GaAs_{1-x}Sb_x$ was well controlled below a 200arcsec separation from the InP substrate peak. This corresponds to a mismatch of less than 1 atomic percentage at $x = 0.487$ to InP.

Figure 4 shows the room temperature hole mobility of the carbon-doped GaAsSb as a function of hole concentration. A hole concentration as high as $1 \times 10^{20} cm^{-3}$ has been achieved. However ,the hole mobility decreases from 46 to $36 cm^2/(V \cdot s)$ as the hole concentration increases from 4.3×10^{19} to $1 \times 10^{20} cm^{-3}$. This shows a weak dependence of the hole mobility at the higher doping level. We attribute the relatively low hole mobility compared to that of InGaAs to strong alloy scattering with the GaAsSb material system[9,10]. Compared to the reported data from MOCVD[10,11] and GSMBE[11] ,favorable hole mobility values were obtained.

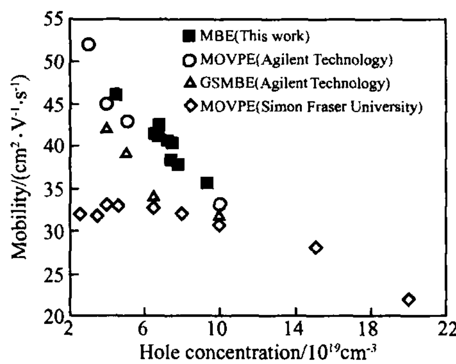

Fig. 4 Hall mobility versus carbon doping level of GaAsSb studied in this paper and previously published papers

3.3 Uniformity

Under normal MBE growth conditions with a unity sticking coefficient for the group Ⅲ elements ,the GaAsSb growth rate is limited by the Ga growth rate. The only unknown is the composition of the mixed group Ⅴ,i. e. the ratio between As and Sb across the platen. From experience ,the Ga growth rate for the Riber 49 under normal platen rotation is within ±1 % across the substrate platen with an approximate shape of a $225 mm^2$. For a Riber 49 with a 4 ×100mm platen configuration , the 100mm substrates are placed symmetrically in a square configuration.

X-ray diffraction is used to quantify the composition uniformity of the 100nm CBr_4-doped GaAsSb epilayer grown on a 100mm semi-insulating InP :Fe substrate in a 4 ×100mm platen. The uniformity of GaAsSb :C is an important criterion for any GaAsSb-based HBT circuit development in the industry.

Non-uniformity in the composition and doping concentration control of the GaAsSb :C will affect the V_{be} of the HBT ,and hence the performance of the HBT circuits. Figure 5 (a) shows the rocking curves of the 100mm GaAsSb :C wafer measured at multiple points across the diameter of the wafer along the radial direction of the platen. The GaAsSb epilayer was purposely grown with a

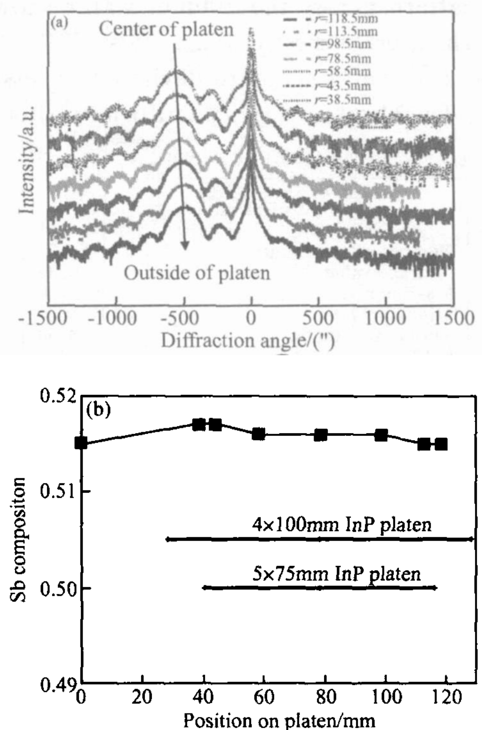

Fig. 5 (a) X-ray rocking curve of GaAsSb material grown at different locations of 4 ×100mm platen; (b) Sb composition distribution from center of platen to the side The fluctuation of Sb atomic composition is less than 0.1 % ,which guarantees uniform distribution of Sb for whole device growth on MBE production system.

lattice mismatch so that the diffraction peak of GaAsSb could be easily distinguished from the InP substrate peak. The GaAsSb diffraction peaks are ~500arcsec away from the InP substrate peak. The measured X-ray spectra are almost identical at each point across the wafer. This indicates that the substrate temperature distribution in the radial direction of the 4 ×100mm platen is uniform. Figure 5 (b) summarizes the compositional uniformity variation of the 100mm GaAsSb ∶C grown on this 4 × 100mm platen. The Sb composition fluctuation is less than ±0.1 atomic percentage across the 100mm wafer and the whole platen. This high composition uniformity assures that 4 × 100mm GaAsSb HBTs can be grown in one growth run, which is very important for the fabrication processing development of HBT circuits and technology.

The uniformity of carbon doping across this 100mm GaAsSb epilayer was measured with the Lehighton sheet resistivity mapping with a 36-point pattern across the 100mm wafer shown in Fig.6. The average sheet resistance was ~347.1Ω/□, with a cross-wafer standard deviation of less than 2.3%. The sheet resistivity uniformity should be

Test File:70030B4BA01_C2_W01.tst Test Time

Statistical summary	
Number of test points	36
Average value	347.0932
Maximum value	360.2149
Minimum value	331.6035
Sample spread(%)	8.63
Std Dev value	8.0469
Wafer uniformity value(%)	2.32

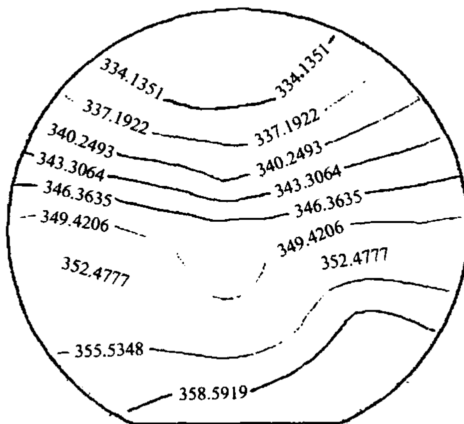

Fig. 6 Leighton resistance distribution of carbon doped GaAsSb material The standard deviation of the resistance is 2.5%, which makes the distribution uniform enough for production growth.

adequate for GaAsSb-based DHBT circuit development. Improvements could be made with further optimization of the CBr_4 injector showerhead.

3.4 InAlAs/ GaAsSb/ InP DHBTs

To further evaluate the material quality of our GaAsSb ∶C grown in our multi-wafer MBE, we explored the growth of InAlAs/ GaAsSb/ InP DHBTs with the help of in-situ ABES and OFM sensors. We were able to reproduce the HBT characteristics from run to run by repeating the ABES growth temperature profile in both InGaAs and GaAsSb-based HBTs. Note that the infrared pyrometer does not work for substrate temperatures much below 500 ℃ for a multi-wafer production MBE reactor. During the low substrate temperature growth, thermal reflection signals from group Ⅲ or dopant cells can easily drown out the actual thermal emission from the substrate.

We further fabricated and tested LADs of InAlAs/ GaAsSb/ InP DHBTs with a 50μm ×50μm emitter mesa. Figure 7 shows the common emitter I_c-V_{ce} curves of an InAlAs/ GaAsSb/ InP DHBT

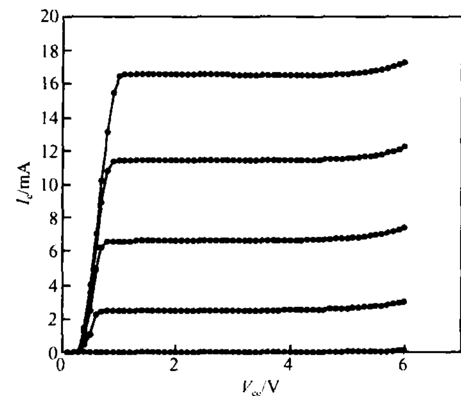

Fig.7 Common emitter I_c-V_{ce} curves of an InAlAs/ GaAsSb/ InP DHBT with 40nm base thickness and 4.5 ×10^{19}cm^{-3} base doping

with 40nm base thickness and 4.5 ×10^{19}cm^{-3} base doping. The InP ∶Si collector thickness is 200nm. The LAD has BV_{ceo} > 6V with a DC current gain of 45 at 1kA/cm^2. The base sheet resistivity is ~1000Ω/□ as measured by the transmission line method (TLM). The collector and base ideality factors are 1.35 and 1.91, respectively. A Gummel plot is shown in Fig. 8. The performance verifies the high quality of the material. After the simple structure test, we further develop the power ampli-

fier structure.

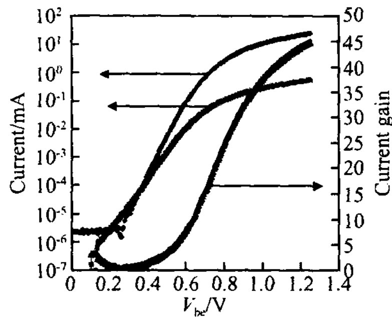

Fig. 8 Gummel plot from InAlAs/ GaAsSb/ InP DHBT with $4.5 \times 10^{19} cm^{-3}$ base doping

The small area devices with a 4μm ×30μm emitter size were fabricated with the power GaAsSb/ InP DHBT epi-structure. The epi-structure is shown in Table 1. Figure 9 is a map of the current gain at $10kA/cm^2$ across the 100mm InP wafer. The gain is 30 ±0.59, which corresponds to a variation of about 2 %, which is consistent with the Sb composition and carbon doping efficiency uniformity mentioned above. Figure 10 is a plot of MSG/ MAG versus frequency, the f_t and f_{max} are both over 50GHz. For comparison, Professor Feng's group at the University of Illinois at Urbana Champaign demonstrated f_t and f_{max} of 350/ 250GHz for high frequency DHBT devices[12]. The reason for the low f_t and f_{max} is that the structure in this paper was designed for power amplifier application and not for high speed. Figure 11 shows f_t versus collector current at different V_{ce} biases.

Table 1 InAlAs/ GaAsSb/ InP power amplifier DHBT structure

Layer	Comment	Material	x	Thickness/ nm	Dopant	Level/ cm^{-3}	Type
9	Cap	$In_xGa_{1-x}As$	0.532	100	Si	3.0×10^{19}	n^+
8	Emitter	InP		20	Si	3.0×10^{19}	n^+
7	Emitter	$In_xAl_{1-x}As$	0.522	30	Si	5.0×10^{17}	n
6	Interfacial	InP		Thin	Si	5.0×10^{17}	n
5	Base	$GaAs_{1-x}Sb_x$	0.487	50	C	6.0×10^{19}	p^+
4	Collector doping spike	InP		9	Si	2.0×10^{17}	n
3	Collector	InP		750	Si	2.0×10^{16}	n
2	Sub-collector	$In_xGa_{1-x}As$	0.532	10	Si	3.0×10^{19}	n^+
1	Sub-collector	InP		400	Si	3.0×10^{19}	n^+

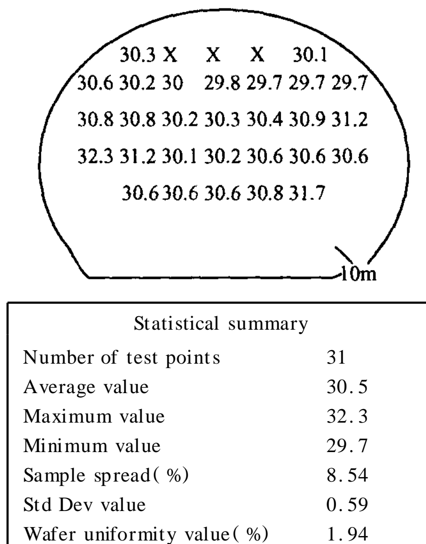

Statistical summary	
Number of test points	31
Average value	30.5
Maximum value	32.3
Minimum value	29.7
Sample spread(%)	8.54
Std Dev value	0.59
Wafer uniformity value(%)	1.94

Fig. 9 Gain distribution across the whole 100mm InP wafer, which confirmed uniform distribution of Sb and carbon cross the whole 100mm InP wafer

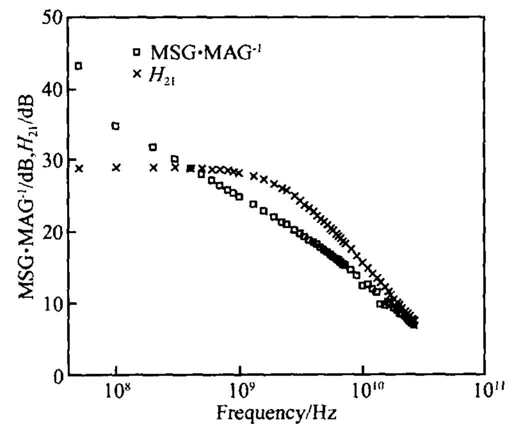

Fig. 10 Plot MSG/ MAG versus frequency The measured f_t and f_{max} are all over 50GHz.

As seen in the figure, the peak f_t stops changing at V_{ce} above 1.5V. This indicates little or no BC junction current blockage as expected from a type-II band alignment for the GaAsSb/ InP BC junction. Figure 12 is the load pull data for this device. The RF gain of 23 is comparable to a GaAs PA HBT at low P_{in}. The peak power amplifier efficiency is 50 %. For comparison, Professor Feng's group at the University of Illinois at Urbana Champaign demonstrated an amplifier efficiency of 41 % at

10GHz for high frequency DHBT devices[13]. Since this work on GaAsSb power amplifier HBT is preliminary, there is still much room for improvement through further optimization of the epi-structure and device processing.

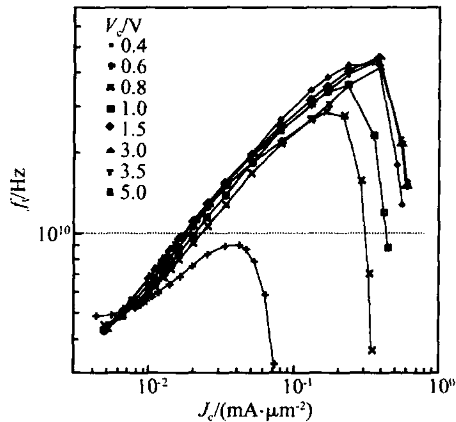

Fig. 11 f_t versus collector current at different V_{ce} biases

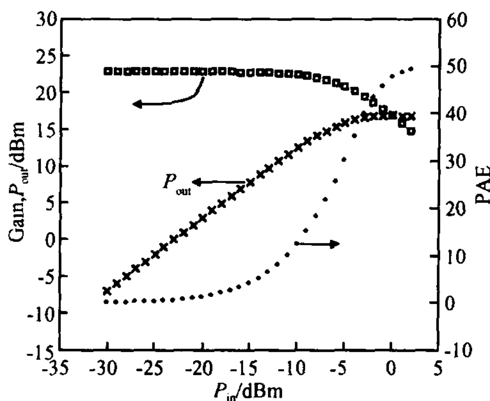

Fig. 12 Load pull data for power amplifier DHBT

4 Conclusion

In summary, we have investigated GaAsSb DHBTs with an InAlAs emitter using multi-wafer production MBE. State-of-the-art hole mobilities were obtained for 100nm thick carbon-doped GaAsSb. We have also demonstrated the Sb composition variation to be less than ±0.1 atomic percentage across a 100mm wafer grown on a 4 × 100mm platen. The uniformity of GaAsSb and the excellent electrical properties of InAlAs/GaAsSb/InP DHBTs demonstrate that the multi-wafer MBE mass production of GaAsSb based DHBTs is feasible. The preliminary power amplifier HBT structure shows similar performance to GaAs PA HBTs and InGaAs/InP PA HBTs.

Acknowledgement The authors would like to thank Dr. Y. K. Chen and N. Weimann from Lucent Technologies for the DARPA-TFAST program management support, as well as DARPA-TFAST program manager Dr. J. C. Zolper for program support. Thanks also to Cristian Cismaru, Peter Zampardi, and Mike Sun from Skyworks Solutions, Inc. for characterization support.

References

[1] Bolognesi C R, Matine N, Dvorak M W, et al. InP/GaAsSb/InP double HBTs: a new alternative for InP-Based DHBTs. IEEE Trans Electron Devices, 2001, 48: 2631

[2] Matine N, Dvorak M W, Lam S, et al. Demonstration of GSMBE grown InP-GaAs$_{0.51}$Sb$_{0.49}$ InP DHBTs. Proc of the International Conf on Indium Phosphide and Related Materials, 2000: 239

[3] Bolognesi C R, Dvorak M W, Matine N, et al. Ultrahigh performance staggered lineup ("Type-Ⅱ") InP/GaAsSb/InP npn double heterojunction bipolar transistors. Jpn J Appl Phys, 2002, 41: 1131

[4] Dvorak M W, Bolognesi C R, Pitts O J, et al. 300GHz InP/GaAsSb/InP double HBTs with high current capability and BV_{CEO} > 6V. IEEE Electron Device Lett, 2001, 22: 361

[5] Johnson S R, Lavoie C, Tiedje T, et al. Semiconductor substrate temperature measurement by diffuse reflectance spectroscopy in molecular beam epitaxy. J Vac Sci Technol B, 1993, 11: 1007

[6] Roth J A, De Lyon T J, Adel M E. In situ substrate temperature measurement during MBE by band-edge reflection spectroscopy. Proc Mater Res Soc Symp, 1994, 324: 353

[7] Pinsukanjana P, Jackson A, Tofte J, et al. Real-time simultaneous optical-based flux monitoring of Al, Ga, and In using atomic absorption for molecular beam epitaxy. J Vac Sci Technol B, 1996, 14: 2147

[8] Pinsukanjana P R, Marquis J M, Hubbard J, et al. InGaAs composition monitoring for production MBE by in situ optical-based flux monitor (OFM). J Cryst Growth, 2003, 251: 124

[9] Cherng M J, Cohen R M, Stringfellow G B. GaAs$_{1-x}$Sb$_x$ growth by OMVPE. J Electron Mater, 1984, 13: 799

[10] Watkins S P, Pitts O J, Dale C, et al. Heavily carbon-doped GaAsSb grown on InP for HBT applications. J Cryst Growth, 2000, 221: 59

[11] Yi S S, Chung S J, Rohdin H, et al. Growth and device performance of InP/GaAsSb HBTs. Proc of the International Conf on Indium Phosphide and Related Materials, 2003: 380

[12] Chu-Kung B F, Feng M. InP/GaAsSb type-Ⅱ DHBTs with f_T > 350GHz. Electron Lett, 2004, 40: 1305

[13] Caruth D C, Chu-Kung B F, Feng M. 10-GHz power performance of a type Ⅱ InP/GaAsSb DHBT. IEEE Electron Device Lett, 2005, 26: 604